

EFFICIENT ORDER-OPTIMAL PRECONDITIONERS FOR IMPLICIT RUNGE–KUTTA AND RUNGE–KUTTA–NYSTRÖM METHODS APPLICABLE TO A LARGE CLASS OF PARABOLIC AND HYPERBOLIC PDES

MICHAEL R. CLINES*, VICTORIA E. HOWLE†, AND KATHARINE R. LONG‡

Abstract. We generalize previous work by Mardal, Nilssen, and Staff (2007, *SIAM J. Sci. Comp.* v. 29, pp. 361–375) and Rana, Howle, Long, Meek, and Milestone (2021, *SIAM J. Sci. Comp.* v. 43, pp. 475–495) on order-optimal preconditioners for parabolic PDEs to a larger class of differential equations and methods. The problems considered are those of the forms $u_t = -\mathcal{K}u + g$ and $u_{tt} = -\mathcal{K}u + g$, where the operator \mathcal{K} is defined by $\mathcal{K}u := -\nabla \cdot (\alpha \nabla u) + \beta u$ and the functions α and β are restricted so that $\alpha > 0$, and $\beta \geq 0$. The methods considered are A-stable implicit Runge–Kutta methods for the parabolic equation and implicit Runge–Kutta–Nyström methods for the hyperbolic equation. We prove the order optimality of a class of block preconditioners for the stage equation system arising from these problems, and furthermore we show that the LD and DU preconditioners of Rana *et al.* are in this class. We carry out numerical experiments on several test problems in this class — the 2D diffusion equation, Pennes bioheat equation, the wave equation, and the Klein–Gordon equation, with both constant and variable coefficients. Our experiments show that these preconditioners, particularly the LD preconditioner, are successful at reducing the condition number of the systems as well as improving the convergence rate and solve time for GMRES applied to the stage equations.

Key words. Preconditioners, Iterative Methods, Implicit Runge–Kutta, Runge–Kutta–Nyström

AMS subject classifications. 65F08, 65N30, 65L06

1. Introduction. Implicit Runge–Kutta (IRK) methods are efficient time integration methods that avoid the Dahlquist barriers that limit the order and stability of implicit multistep methods. A disadvantage of IRK methods has been the lack of effective preconditioners for the resulting linear systems; however, some progress has been made. In [8], Mardal *et al.* proved order optimality of a class of block diagonal preconditioners for parabolic equations, where order optimality means that the condition number of the preconditioned system is bounded independently of the timestep h_t and the mesh size h_x . In [12], Rana *et al.* developed a preconditioner based on a block LDU factorization that showed excellent performance on the diffusion and advection-diffusion equations; however, order optimality of their preconditioner was not proved.

In this paper, we generalize the analysis of [8] to prove order optimality for a class of preconditioners for IRK systems arising from a family of parabolic and hyperbolic partial differential equations that includes the diffusion, Pennes bioheat[11], wave, and Klein–Gordon equations. In particular, we prove that the LD and DU preconditioners of Rana *et al.* are order optimal for all equations in this family.

Let Ω be a bounded polygonal region in \mathbb{R}^d with boundary $\partial\Omega$ partitioned into disjoint subsets $\partial\Omega_N$ and $\partial\Omega_D$. Let μ be either 1 or 2, and let $\alpha(\mathbf{r})$, $\beta(\mathbf{r})$, $g(\mathbf{r}, t)$, $u_0(\mathbf{r})$, and $\dot{u}_0(\mathbf{r})$ be real-valued functions, with α and β subject to the conditions $\alpha(\mathbf{r}) >$

* (Corresponding author) Department of Mathematics and Statistics, Texas Tech University, Lubbock Texas, USA,

† Department of Mathematics and Statistics, Texas Tech University, Lubbock Texas, USA,

‡ Department of Mathematics and Statistics, Texas Tech University, Lubbock Texas, USA

0, $\beta(\mathbf{r}) \geq 0 \forall \mathbf{r} \in \Omega$. We define the linear differential operator \mathcal{K} by

$$\mathcal{K}u := -\nabla \cdot (\alpha \nabla u) + \beta u.$$

We focus on the linear initial-boundary value problem

$$(1.1) \quad \frac{\partial^\mu u}{\partial t^\mu} = -\mathcal{K}u + g \quad \text{in } \Omega \text{ for } t > 0$$

$$(1.2) \quad \alpha \hat{\mathbf{n}} \cdot \nabla u = 0 \quad \text{on } \partial\Omega_N; \quad u = 0 \quad \text{on } \Omega_D$$

with initial conditions

$$(1.3) \quad u(\mathbf{r}, 0) = u_0(\mathbf{r})$$

and, if $\mu = 2$,

$$(1.4) \quad u_t(\mathbf{r}, 0) = \dot{u}_0(\mathbf{r}).$$

With $\mu = 1$ we have the diffusion ($\beta = 0$) and Pennes bioheat ($\beta > 0$) equations, while with $\mu = 2$ we have the wave ($\beta = 0$) and Klein–Gordon ($\beta > 0$) equations.

Time discretization will be done with an IRK method when $\mu = 1$, and with an implicit Runge–Kutta–Nyström (IRKN) method when $\mu = 2$; these methods are briefly reviewed in section 2.1. In subsection 2.1.2 we present a unified formulation of the Galerkin weak forms of the stage equations for IRK and IRKN methods. From this we develop a continuous boundary value problem $\mathcal{A}\mathbf{k} = \mathbf{f}$ that must be solved at every timestep for the stage variables \mathbf{k} ; when this problem is discretized in space with finite elements, we obtain a linear system of equations. It is that linear system we are concerned with preconditioning.

Following [8], in section 3 we study the continuous form of the stage equations to show that the mapping \mathcal{A} is an isomorphism, and we apply that analysis to study order-optimality of block preconditioners. Results of numerical experiments are presented in section 4, and then conclusions and future directions are discussed in section 5.

2. Time and space discretization. For the remainder of this paper, vector-valued functions and spaces of vector-valued functions are denoted by bold face symbols. The L^2 inner product and its induced norm are defined as usual as

$$\langle u, v \rangle_{L^2} := \int_{\Omega} uv \, d\Omega; \quad \|u\|_{L^2} := \sqrt{\langle u, u \rangle_{L^2}}.$$

For a Sobolev inner product and norm we take

$$\langle u, v \rangle_{H_0^1} := \int_{\Omega} \alpha \nabla u \cdot \nabla v + \beta uv \, d\Omega; \quad \|u\|_{H_0^1} := \sqrt{\langle u, u \rangle_{H_0^1}},$$

where $h_t > 0$ is a timestep. In the corner case where $\beta = 0$ and $\Omega_D = \emptyset$, our Sobolev inner product is not a true inner product, and its norm is only a seminorm; however, we will soon see that this is ultimately irrelevant because these operations won't be used alone, so we tolerate this abuse of notation. With a number of Runge–Kutta stages $s \in \mathbb{N}$, we define the spaces

$$V := L^2(\Omega) \cap H_0^1(\Omega),$$

$$\mathbf{V} := V^s = (V \times \cdots \times V) = \mathbf{L}^2(\Omega) \cap h_t^\mu \mathbf{H}_0^1(\Omega),$$

where \otimes is the Cartesian product of vector spaces. The inner products and norms in these spaces are

$$\begin{aligned}\langle u, v \rangle_V &:= \langle u, v \rangle_{L^2} + h_t^\mu \langle u, v \rangle_{H_0^1}; & \|u\|_V &= \sqrt{\|u\|_{L^2}^2 + h_t^\mu \|u\|_{H_0^1}^2} \\ \langle \mathbf{u}, \mathbf{v} \rangle_{\mathbf{V}} &:= \langle \mathbf{u}, \mathbf{v} \rangle_{\mathbf{L}^2} + h_t^\mu \langle \mathbf{u}, \mathbf{v} \rangle_{\mathbf{H}_0^1}; & \|\mathbf{u}\|_{\mathbf{V}} &= \sqrt{\|\mathbf{u}\|_{\mathbf{L}^2}^2 + h_t^\mu \|\mathbf{u}\|_{\mathbf{H}_0^1}^2}.\end{aligned}$$

These inner products and norms on V and \mathbf{V} are true inner products and norms even in the corner case where $\|\cdot\|_{H_0^1}$ is only a seminorm. Note that for the L^2 , H_0^1 , and V inner products, the vectorized inner products $\langle \mathbf{u}, \mathbf{v} \rangle$ are related to the inner products $\langle u, v \rangle$ by

$$\langle \mathbf{u}, \mathbf{v} \rangle = \sum_{i=1}^s \langle u_i, v_i \rangle.$$

We will remove the space specification whenever it is clear which inner product is being used. The operator \mathcal{K} applied to a vector \mathbf{u} is to be interpreted such that $(\mathcal{K}\mathbf{u})_i = \mathcal{K}u_i$.

2.1. Implicit Runge–Kutta methods. An IRK method with s stages is specified by its Butcher coefficients $A \in \mathbb{R}^{s \times s}$, $b \in \mathbb{R}^s$, $c \in \mathbb{R}^s$. Throughout this paper we assume that we are working with an A-stable IRK or IRKN method. For all such methods, the matrix A will be nonsingular and irreducible. With IRKN methods based on indirect collocation (see, *e.g.*, [3, 4]), the Butcher matrix A is formed as $A = \hat{A}\hat{A}$, where \hat{A} is the matrix from a base IRK method. Our analysis will rely on the matrix A being weakly positive definite [8, 9]. We have confirmed this assumption through numerical experiments by examining the spectrum of all the IRK and IRKN methods considered here.

Since the focus of timestepping methods is on the time variable, in the following discussion we don't show explicitly the dependence on spatial position \mathbf{r} ; for example, we write $g(\mathbf{r}, t)$ as $g(t)$ and $u^n(\mathbf{r})$ simply as u^n .

The numerical solution at step $n - 1$ is advanced to step n by the step formula

$$\begin{aligned}t^n &= t^{n-1} + h_t \\ u^n &= u^{n-1} + h_t \sum_{i=1}^s b_i k_i^n,\end{aligned}$$

where the stage variables $k_i^n : \Omega \rightarrow \mathbb{R}$, $i = 1 : s$, are computed by solving the stage equations

$$k_i^n = -\mathcal{K} \left(u^{n-1} + h_t \sum_{j=1}^s a_{ij} k_j^n \right) + g(t^{n-1} + c_i h_t); \quad i = 1 : s,$$

with homogeneous boundary conditions on each k_i^n . The stage equations are a set of s coupled boundary value problems.

2.1.1. IRK–Nyström methods. Runge–Kutta–Nyström methods are an extension of Runge–Kutta methods suitable for second-order differential equations. A second set of weights, $b' \in \mathbb{R}^s$, is used so that the step formulas for advancing the

solution u^n and the time derivative \dot{u}^n are

$$\begin{aligned} u^n &= u^{n-1} + h_t \dot{u}^{n-1} + h_t^2 \sum_{i=1}^s b_i k_i^n \\ \dot{u}^n &= \dot{u}^{n-1} + h_t \sum_{i=1}^s b'_i k_i^n. \end{aligned}$$

The stage variables k_i^n are found by solving

$$k_i^n = -\mathcal{K} \left(u^{n-1} + h_t c_i \dot{u}^{n-1} + h_t^2 \sum_{j=1}^s a_{ij} k_j^n \right) + g(t^{n-1} + c_i h_t); \quad i = 1 : s,$$

with homogeneous boundary conditions. Note that although the equation is second order in time, with a RKN method there are only s , not $2s$, stage equations to be solved.

2.1.2. A unified formulation of the IRK and IRKN stage equations.

Observe that we can easily express the stage equations for both IRK (with $\mu = 1$) and IRKN ($\mu = 2$) in the unified form

$$k_i^n = -\mathcal{K} \left(u^{n-1} + (\mu - 1) h_t c_i \dot{u}^{n-1} + h_t^\mu \sum_{j=1}^s a_{ij} k_j^n \right) + g(t^{n-1} + c_i h_t).$$

The time derivatives \dot{u}^n are never needed when $\mu = 1$. If we introduce the variable

$$(2.1) \quad f_i^n = g(t^n + c_i h_t) + u^{n-1} + (\mu - 1) h_t c_i \dot{u}^{n-1},$$

then the i -th stage equation becomes

$$(2.2) \quad k_i^n + h_t^\mu \sum_{j=1}^s a_{ij} \mathcal{K} k_j^n = f_i^n.$$

As a final notational simplification, introduce the vector of stage variables

$$\mathbf{k}^n = \begin{bmatrix} k_1^n & k_2^n & \cdots & k_s^n \end{bmatrix}^T,$$

the vector $\mathbf{f}^n = \begin{bmatrix} f_1^n & f_2^n & \cdots & f_s^n \end{bmatrix}^T$, the $s \times s$ identity matrix $\mathbb{I}^{s \times s}$, and the identity operator $\mathcal{I} : V \rightarrow V$. Then the system of stage equations is written compactly as

$$(\mathbb{I}^{s \times s} \otimes \mathcal{I} + h_t^\mu A \otimes \mathcal{K}) \mathbf{k}^n = \mathbf{f}^n,$$

where \otimes is the Kronecker product. We can also define $\mathcal{A} : \mathbf{V} \rightarrow \mathbf{V}^*$ as

$$(2.3) \quad \mathcal{A} := \mathbb{I}^{s \times s} \otimes \mathcal{I} + h_t^\mu A \otimes \mathcal{K},$$

in which case the equation to be solved is simply

$$(2.4) \quad \mathcal{A} \mathbf{k}^n = \mathbf{f}^n.$$

2.2. Finite element discretization. We now develop a variational form of the stage equations. Begin by observing that for all $v \in V$, we have

$$\int_{\Omega} v \mathcal{K} u \, d\Omega = \int_{\Omega} \alpha \nabla u \cdot \nabla v + \beta uv \, d\Omega = \langle v, u \rangle_{H_0^1}.$$

Now assert an orthogonal residual condition with test function $v_i \in V$ on equation 2.2, obtaining

$$(2.5) \quad \langle k_i^n, v_i \rangle_{L^2} + h_t^\mu \sum_{j=1}^s a_{ij} \langle k_j^n, v_i \rangle_{H_0^1} = \langle f_i^n, v_i \rangle_{L^2}.$$

Choose an N -dimensional approximating subspace $\mathbf{V}_h \subset \mathbf{V}$, where $h > 0$ is a notational representation of the mesh size. Quantities with subscript h are discretized in this space; for example, the function $k_{i,h}^n \in V_h$ will be the i -th discrete stage variable at timestep n . The vectorized discrete space is $\mathbf{V}_h = (V_h)^s$. Let $\{\phi_\ell\}_{\ell=1}^N$ be a basis for V_h , and form the matrices $M \in \mathbb{R}^{N \times N}$ and $F \in \mathbb{R}^{N \times N}$ with entries

$$(2.6) \quad M_{\ell m} := \langle \phi_\ell, \phi_m \rangle_{L^2}$$

$$(2.7) \quad F_{\ell m} := \langle \mathcal{K} \phi_m, \phi_\ell \rangle_{L^2} = \langle \alpha \nabla \phi_m, \nabla \phi_\ell \rangle_{L^2} + \langle \beta \phi_m, \phi_\ell \rangle_{L^2} = \langle \phi_m, \phi_\ell \rangle_{H_0^1}$$

and the vector $f_{i,h}^n \in \mathbb{R}^N$ with entries

$$(2.8) \quad (f_{i,h}^n)_\ell = \langle f_i^n, \phi_\ell \rangle_{L^2}.$$

The i -th stage equation from (2.5) then becomes

$$M k_{i,h}^n + h_t^\mu \sum_{j=1}^n a_{ij} F k_{j,h}^n = f_{i,h}^n,$$

and the full system in vectorized notation is

$$(2.9) \quad (\mathbb{I}^{s \times s} \otimes M + h_t^\mu A \otimes F) \mathbf{k}_h^n = \mathbf{f}_h^n.$$

The matrix on the left hand side is the discretization of the operator \mathcal{A} , so we denote it as \mathcal{A}_h ,

$$\mathcal{A}_h = \mathbb{I}^{s \times s} \otimes M + h_t^\mu A \otimes F.$$

3. Analysis of the continuous stage equations and preconditioner. We now analyze the continuous form of the stage equations (2.4)

$$\mathcal{A} \mathbf{k}^n = \mathbf{f}^n,$$

where the operator $\mathcal{A} : \mathbf{V} \mapsto \mathbf{V}^*$ has been defined in (2.3),

$$\mathcal{A} := \mathbb{I}^{s \times s} \otimes \mathcal{I} + h_t^\mu A \otimes \mathcal{K}.$$

We note the similarity to the stage equation operator $\mathcal{A} := I - h_t A \otimes \nabla^2$ considered in [8]. We therefore follow the path laid out by [8]: we establish that \mathcal{A} is an isomorphism given certain assumptions about the Butcher coefficient matrix A , and obtain the following theorem.

THEOREM 3.1. *Let $A \in \mathbb{R}^{s \times s}$ be weakly positive definite, and let $h_t > 0$, $\mu \in \{1, 2\}$. Then the operator $\mathcal{A} = \mathbb{I}^{s \times s} \otimes \mathcal{I} + h_t^\mu A \otimes \mathcal{K}$ is an isomorphism, and there exist finite constants c_1, c_2 , independent of the timestep h_t , such that*

$$\begin{aligned} \|\mathcal{A}\|_{\mathcal{L}(\mathbf{V}, \mathbf{V}^*)} &\leq c_1 \\ \|\mathcal{A}^{-1}\|_{\mathcal{L}(\mathbf{V}^*, \mathbf{V})} &\leq c_2. \end{aligned}$$

Because the proof is a straightforward extension of that found in [8], we leave the proof to Appendix A.

Now consider a continuous preconditioner of the form

$$(3.1) \quad \mathcal{P} = I + h_t^\mu P \otimes \mathcal{K},$$

where P is a weakly positive definite matrix; this is simply the operator \mathcal{A} but with the Butcher matrix A replaced by an approximation P that has preserved the weakly positive definiteness of A . From Theorem 3.1 we see immediately that \mathcal{P} is an isomorphism. Since \mathcal{P} is an isomorphism between \mathbf{V} and \mathbf{V}^* , its inverse \mathcal{P}^{-1} exists and maps \mathbf{V}^* to \mathbf{V} , and from Theorem 3.1 we have the bounds

$$\|\mathcal{P}\| \leq d_1; \quad \|\mathcal{P}^{-1}\| \leq d_2.$$

Furthermore, the composition $\mathcal{P}^{-1}\mathcal{A} : \mathbf{V} \rightarrow \mathbf{V}$ is also an isomorphism with bounds

$$\|\mathcal{P}^{-1}\mathcal{A}\| \leq c_1 d_2 \text{ and } \|\mathcal{A}^{-1}\mathcal{P}\| \leq c_2 d_1.$$

From this we immediately establish a bound on the condition number of the continuous left-preconditioned operator $\mathcal{P}^{-1}\mathcal{A}$ that is independent of our choice of h_t , that is,

$$\kappa(\mathcal{P}^{-1}\mathcal{A}) = \|\mathcal{P}^{-1}\mathcal{A}\| \|\mathcal{A}^{-1}\mathcal{P}\| \leq c_1 d_2 c_2 d_1.$$

Hence this family of preconditioners is a set of order optimal preconditioners with respect to time. Next we establish that these preconditioners are also order optimal with respect to the discretization parameter h .

We now consider the following discrete subspaces

$$V_h \subset V \quad \text{and} \quad \mathbf{V}_h = (V_h)^s \subset \mathbf{V}.$$

The discretized versions \mathcal{A}_h and \mathcal{P}_h of the above continuous operators \mathcal{A} and \mathcal{P} are given by

$$(3.2) \quad \mathcal{A}_h := \mathbb{I}^{s \times s} \otimes M + h_t^\mu A \otimes F$$

$$(3.3) \quad \mathcal{P}_h := \mathbb{I}^{s \times s} \otimes M + h_t^\mu P \otimes F,$$

where F, M are the stiffness and mass matrices, respectively. Since $\mathbf{V}_h \subset \mathbf{V}$, we obtain

$$\kappa(\mathcal{P}_h^{-1}\mathcal{A}_h) \leq \kappa(\mathcal{P}^{-1}\mathcal{A}) \leq c_1 d_2 c_2 d_1,$$

showing that $\mathcal{P}^{-1}\mathcal{A}$ is bounded independently of the discretization parameter h . We conclude that the preconditioner \mathcal{P} is order optimal with respect to both timestep h_t and spatial discretization parameter h .

Now that we have established that any preconditioner \mathcal{P} with P weakly positive definite is order-optimal, we now focus on several examples of interest. We can define a

few particular instances of this preconditioner based on our selection of P , specifically where P is a preconditioner for the Butcher coefficient matrix A arising from our choice of timestepper.

The motivation behind this decision comes from the observation that $\kappa(\mathcal{P}^{-1}\mathcal{A}) \propto \kappa(P^{-1}A)$ for $\beta = 0$, as established in [13], [8], and [12]. In other words, if we can construct \mathcal{P} such that P is a good preconditioner for A , then \mathcal{P} is likely to be a good preconditioner for \mathcal{A} . Some simple examples are the block Jacobi and block Gauss-Seidel preconditioners studied by [13, 8] and the LDU-factorization preconditioners introduced in [12]. Additionally, we will also show the results of using the upper triangular part of A , namely \mathcal{P}_{TRIU} .

The order optimality of \mathcal{P}_{LD} and \mathcal{P}_{DU} was suggested experimentally, but not proved, by [12]. All five of these preconditioners are easily constructed and applied; the factorizations in the LD and DU preconditioners are done on the small Butcher coefficient matrices A , not on the full matrix \mathcal{A}_h . We have numerically verified the weak positive definiteness of all the above preconditioners. See Appendix B for the specific definition of each preconditioner.

4. Numerical Experiments. We conduct a series of numerical experiments to investigate the behavior of several preconditioners in problems of the type considered in this paper. Left preconditioning is used throughout. In all experiments, homogeneous Neumann boundary conditions are used and spatial discretization is done with Galerkin finite elements using first-degree Lagrange basis functions on a 2D triangular mesh. For each problem, we consider both constant and non-constant coefficients. For the constant coefficient experiments, we set $\alpha = \beta = 1$, and for the variable coefficient experiments we use

$$\begin{aligned}\alpha(\mathbf{r}) &:= 1 + 0.2xy \\ \beta(\mathbf{r}) &:= 1 + 0.3 \sin(\pi x) \cos(\pi y)\end{aligned}$$

On the domain $\Omega = [-1, 1] \times [-1, 1]$ these functions are strictly positive.

For parabolic problems, the Radau IIA method is used; for the hyperbolic problems, an IRKN method based on the Gauss–Legendre method is used. Unless otherwise specified, the timestep h_t is chosen to depend on the mesh size h so that the spatial interpolation error and temporal global truncation error are of comparable magnitude [12]; we set $h_t = h^{\frac{p+1}{q}}$ where p is the degree of the basis polynomials, q is $2s$ for Gauss–Legendre timestepping and $q = 2s - 1$ for Radau IIA timestepping.

In GMRES calculations, the method of manufactured solutions is used to construct exact solutions so that we can calculate relative errors as well as relative residuals.

The matrices M and F are assembled using the Sundance finite element toolkit [7]; when doing solves, the full matrices \mathcal{A}_h are never assembled as all matrix-vector multiplications and diagonal subsolves can be carried out using only M and F . Other than the assembly of M and F , all computations were implemented in Python using the open source packages SciPy[5] and PyAMG[2] on a machine with an AMD Ryzen 7 3800 3.89GHz processor and 16GB of RAM.

4.1. Constant coefficient problems. Our first set of calculations is done using constant coefficients. We compute condition numbers for the constant coefficient preconditioned wave and Klein–Gordon equations as functions of h , h_t and s and for

GL-(s)	$\kappa(\mathcal{A})$	$\kappa(\mathcal{P}_J^{-1}\mathcal{A})$	$\kappa(\mathcal{P}_{GSL}^{-1}\mathcal{A})$	$\kappa(\mathcal{P}_{LD}^{-1}\mathcal{A})$	$\kappa(\mathcal{P}_{DU}^{-1}\mathcal{A})$	$\kappa(\mathcal{P}_{TRIU}^{-1}\mathcal{A})$
$h = 2^{-4}$						
GL-2	68.22	17.43	4.39	2.06	7.68	20.46
GL-3	410.88	389.36	43.73	4.80	233.82	595.84
GL-4	966.05	395.42	656.31	5.41	314.39	481.09
GL-5	1807.02	1023.39	753.04	8.01	1145.59	1377.70
$h = 2^{-5}$						
GL-2	105.40	18.91	4.55	2.12	8.15	22.07
GL-3	802.25	413.53	45.88	6.03	244.96	630.85
GL-4	2276.20	484.52	738.48	6.32	414.06	588.11
GL-5	4676.51	1295.65	893.63	9.62	1432.78	1443.22

Table 4.1: Condition numbers of left-preconditioned matrices with preconditioners Jacobi, Gauss–Seidel, LD , DU , and Upper Triangular, with spatial discretization sizes $h = 2^{-4}$, 2^{-5} applied to a 2D wave equation with constant coefficients with s -stage Gauss–Legendre. The time-steps are given by $h_t = h^{\frac{p+1}{q}}$ where $p = 1$ is the degree of the Lagrange polynomial basis functions in space and q is the order of the method ($2s$ for Gauss–Legendre).

a variety of preconditioners (subsection 4.1.1); eigenvalue spectra for the preconditioned constant-coefficient wave equation (subsection 4.1.2); and field of values for the preconditioned constant-coefficient Klein–Gordon equation (subsection 4.1.3).

Condition numbers for the preconditioned diffusion equation with constant coefficients have already been investigated extensively in [8, 13, 12], so we don’t repeat that analysis here. We defer experiments on the diffusion and Pennes equations until our investigation of variable coefficient problems.

4.1.1. Conditioning for the wave and Klein–Gordon equations. Table 4.1 shows calculated condition numbers of the system matrix \mathcal{A}_h arising from the discretized wave equation, constructed with mesh sizes $h = 2^{-4}$, 2^{-5} and then preconditioned with \mathcal{P}_J , \mathcal{P}_{GSL} , \mathcal{P}_{LD} , \mathcal{P}_{DU} , and \mathcal{P}_{TRIU} . The time step is defined to be $h_t = h^{\frac{2}{2s}}$, as specified above. The timestepping methods chosen are the s -stage IRKN Gauss–Legendre methods where s varies from 2–5.

For $s = 2$, all preconditioners reduce the condition number by a factor between 2.5 and 50. As s is increased, we see a sharp rise in the condition number of the original system, and we see an increase in the condition number of the systems preconditioned with $\mathcal{P}_J, \mathcal{P}_{GSL}, \mathcal{P}_{DU}$, and \mathcal{P}_{TRIU} . However, \mathcal{P}_{LD} maintains a consistently small condition number, growing only by $\sim 4 - 5$ as stage number increases and staying under 10 for all h and s considered.

Table 4.2 shows the results of preconditioning the Klein–Gordon equation (with constant coefficients) with $h = 2^{-5}$ held fixed, and with timesteps $h_t = 5.0, 0.5, 0.005$ advanced with Gauss–Legendre 2–5. All preconditioners reduce κ by an order of magnitude or more, with \mathcal{P}_{LD} superior except at the smallest timesteps, where \mathcal{P}_{GSL} is slightly better. It is worth noting that as $h_t \rightarrow 0$, the original system \mathcal{A} converges to a block diagonal mass matrix, which is easily handled by any preconditioner; indeed,

GL-(s)	$\kappa(\mathcal{A})$	$\kappa(\mathcal{P}_J^{-1}\mathcal{A})$	$\kappa(\mathcal{P}_{GSL}^{-1}\mathcal{A})$	$\kappa(\mathcal{P}_{LD}^{-1}\mathcal{A})$	$\kappa(\mathcal{P}_{DU}^{-1}\mathcal{A})$	$\kappa(\mathcal{P}_{TRIU}^{-1}\mathcal{A})$
$h_t = 5.0$						
GL-2	24,776	29.03	8.31	3.38	9.65	36.08
GL-3	70,447	1790.89	180.33	6.10	873.32	2857.00
GL-4	251,624	3025.13	6495.80	33.89	1634.59	3621.96
GL-5	469,410	12,133.55	63,830.62	82.16	10,919.53	15,574.36
$h_t = .5$						
GL-2	3859.26	73.96	9.81	4.27	32.63	78.77
GL-3	6267.10	786.89	89.95	11.77	534.50	1168.69
GL-4	7644.23	653.50	926.44	9.11	75.06	796.45
GL-5	9347.42	1524.38	9678.74	11.33	1915.84	1936.84
$h_t = .005$						
GL-2	438.43	2.43	1.10	1.39	2.39	2.57
GL-3	468.61	3.74	1.77	1.92	3.75	3.96
GL-4	526.19	2.92	1.02	1.65	2.98	2.92
GL-5	529.67	2.97	1.02	1.71	2.99	2.97

Table 4.2: Condition numbers of left-preconditioned matrices with preconditioners Jacobi, Gauss–Seidel, LD , DU , and Upper Triangular, with time step sizes $h_t = 5.0, 0.5, 0.005$ and $h = 2^{-5}$ applied to a 2D Klein–Gordon equation with constant coefficients with s -stage Gauss–Legendre.

all five preconditioners considered perform well at $h_t = 0.005$.

4.1.2. Spectrum of preconditioned wave equation. It is well known that when it comes to preconditioning the iterative solver GMRES, the condition number alone does not necessarily predict a preconditioner’s effectiveness.

Generally, it is desirable to cluster the eigenvalues away from 0. In Figure 4.1, we show the spectrum of the preconditioned wave equation with constant coefficients, spatial discretization size $h = 2^{-4}$, and time step $h_t = h^{\frac{1}{s}}$, coupled with the Gauss–Legendre method of stages 3–5. The three rows contain results for the three stages, with s decreasing downwards. The left column of figures shows the spectrum of the block lower triangular preconditioned (\mathcal{P}_{GSL} and \mathcal{P}_{LD}) systems and the right shows the spectrum of the block upper triangular (\mathcal{P}_{DU} and \mathcal{P}_{TRIU}) preconditioned systems. The spectrum of the unpreconditioned system is also shown, in black. As we can see in all the cases, the eigenvalues of the original systems are clustered near 0 while the preconditioners \mathcal{P}_{LD} and \mathcal{P}_{DU} tend to cluster their eigenvalues near 1, with LD achieving the better clustering of the two.

4.1.3. Field of values for preconditioned Klein–Gordon equation. The field of values (FOV), or numerical range, can also indicate the behavior of a GMRES preconditioner [6]. Since one of the standard worst-case error bounds on GMRES is given by the distance of the boundary of the FOV to the origin [6], in Figure 4.2 we show several plots depicting the numerical range of \mathcal{A} for the Klein–Gordon equation with constant coefficients. The mesh size $h = 2^{-4}$ and time step $h_t = h^{\frac{1}{s}}$ with Gauss–

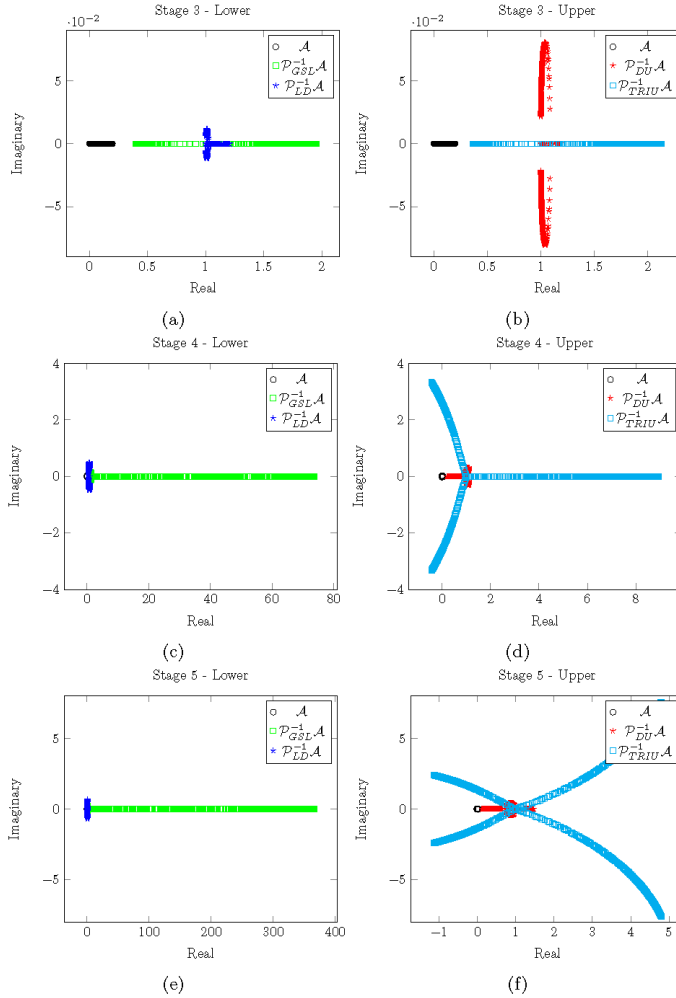


Figure 4.1: Eigenvalues of the left-preconditioned matrices arising from a 2D wave equation, with $h = 2^{-4}$ and using Gauss–Legendre with stages: (a-b) $s = 3$, (c-d) $s = 4$, and (e-f) $s = 5$. The x -axis and y -axis are the real and imaginary axes, respectively. The left column of figures show eigenvalues for the lower triangular preconditioned systems, and the right column of figures shows eigenvalues for the upper triangular preconditioned systems.

Legendre-2 and Gauss–Legendre-3 are used to create the figures. It is clear from these results that \mathcal{P}_{GSL} and \mathcal{P}_{LD} have tighter numerical ranges (smaller distance from zero) than the upper-triangular preconditioned systems, and that \mathcal{P}_{LD} produces a tighter numerical range than \mathcal{P}_{GSL} .

4.2. Variable coefficient problems.

4.2.1. Condition numbers for the diffusion and Pennes equations. Next we consider conditioning of the preconditioned diffusion and Pennes bioheat equations.

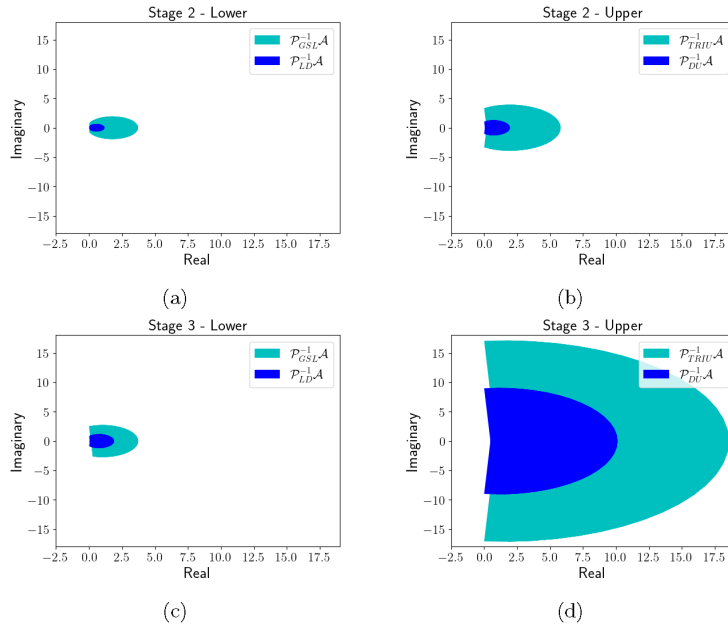


Figure 4.2: Numerical range in the complex plane of preconditioned matrices arising from a Klein–Gordon equation with simplified coefficients, with $h = 2^{-4}$, and using Gauss–Legendre with stages: (a-b) $s = 2$ and (c-d) $s = 3$. The left column of figures shows the lower triangular preconditioned systems, and the right column of figures shows the upper triangular preconditioned systems.

In this set of experiments, we discretize our domain with mesh size $h = 2^{-4}$, and use time steps $h_t = h^{\frac{2}{2s-1}}$, where s is the stage number for the IRK Radau IIA method. As these problems are parabolic, an L-stable method should be used. We follow [8, 12, 13] in choosing the Radau IIA method.

Condition numbers were computed for these problems with the *GSL*, *LD*, and *DU* preconditioners. All three perform remarkably well, with *LD* performing consistently best, and with *GSL* as a runner-up. We also note that the variable coefficients appear to have a minimal impact on the condition number, hence the small variations between the two sets of data.

4.2.2. Condition numbers for the wave and Klein–Gordon equations.

We now repeat the experiments from subsection 4.2.1, changing the equations to the diffusion and Klein–Gordon problems and the timestepper to Gauss–Legendre IRKN. In this case, we see once again that the variable coefficients have little effect on the condition numbers. A difference between these problems and the parabolic problems is that the *GSL* and *DU* preconditioners are ineffective at $s \geq 4$ while the *LD* preconditioner remains effective at all stage numbers.

4.3. Performance of preconditioned GMRES. The acid test of a preconditioner is of course its performance in a solve. Now we investigate the effect of our top three preconditioners in reducing the number of iterations and time required for GMRES to converge to a solution. As mentioned above, we employ the method of

RIIA	$\kappa(\mathcal{A})$	$\kappa(\mathcal{P}_{GSL}^{-1}\mathcal{A})$	$\kappa(\mathcal{P}_{LD}^{-1}\mathcal{A})$	$\kappa(\mathcal{P}_{DU}^{-1}\mathcal{A})$
Diffusion ($\beta = 0$)				
RIIA - 2	973.90	2.99	1.67	24.20
RIIA - 3	3372.07	7.51	2.48	84.65
RIIA - 4	5743.65	15.89	3.11	174.67
RIIA - 5	8280.81	30.27	3.86	306.03
Pennes ($\beta > 0$)				
RIIA - 2	964.09	2.98	1.65	23.76
RIIA - 3	3286.59	7.44	2.43	82.01
RIIA - 4	5693.23	15.68	2.27	81.32
RIIA - 5	8070.54	29.95	3.77	297.37

Table 4.3: Condition numbers of left-preconditioned matrices with preconditioners Gauss–Seidel, LD , and DU with spatial discretization size $h = 2^{-4}$ applied to 2D diffusion and Pennes equations with variable coefficients with s -stage Radau IIA. The time-steps are given by $h_t = h^{\frac{2}{2s-1}}$.

GL	$\kappa(\mathcal{A})$	$\kappa(\mathcal{P}_{GSL}^{-1}\mathcal{A})$	$\kappa(\mathcal{P}_{LD}^{-1}\mathcal{A})$	$\kappa(\mathcal{P}_{DU}^{-1}\mathcal{A})$
$\beta = 0$				
GL-2	167.67	5.50	2.72	15.04
GL-3	691.58	74.71	8.32	467.92
GL-4	1906.88	1049.11	9.70	994.91
GL-5	3923.20	1776.26	16.09	3503.47
$\beta > 0$				
GL-2	167.61	5.50	2.71	15.01
GL-3	691.71	76.61	8.22	467.01
GL-4	1906.73	1048.58	9.67	992.46
GL-5	3922.59	1771.11	16.04	6495.71

Table 4.4: Condition numbers of left-preconditioned matrices with preconditioners Gauss–Seidel, LD , and DU with spatial discretization size $h = 2^{-4}$ applied to 2D wave and Klein–Gordon equations with variable coefficients with s -stage Gauss–Legendre. The time-steps are given by $h_t = h^{\frac{1}{s}}$.

manufactured solutions in order to examine the relative error norms rather than just the residuals. For all of the experiments, a relative residual tolerance for GMRES is set to 10^{-8} . For each stage- s method (where $s = 2 \dots 5$), we examine the iteration count and solve time for each preconditioner, in addition to the resulting relative error.

Rather than apply the preconditioners exactly, we employ the same strategy as that in [8, 13, 12]. Due to the design of the matrices (either block lower triangular or block

RIIA	h	$\mathcal{P}_{GSL}^{-1}\mathcal{A}$			$\mathcal{P}_{LD}^{-1}\mathcal{A}$			$\mathcal{P}_{DU}^{-1}\mathcal{A}$		
		it.	t	err	it.	t	err	it.	t	err
s=2	2^{-5}	11	0.21	8.0e-10	5	0.09	8.9e-9	6	0.12	1.5e-9
	2^{-6}	8	0.83	1.1e-8	7	0.68	4.5e-10	7	0.68	2.7e-10
s=3	2^{-5}	13	0.48	2.1e-9	9	0.38	6.4e-10	10	0.41	4.7e-9
	2^{-6}	11	1.56	8.2e-9	8	1.24	1.7e-9	10	1.47	4.9e-9
s=4	2^{-5}	19	0.97	1.1e-9	10	0.57	4.3e-9	16	0.85	1.4e-9
	2^{-6}	16	2.91	4.2e-9	10	2.05	1.5e-9	14	2.72	4.0e-9
s=5	2^{-5}	19	1.26	3.9e-9	11	0.81	5.2e-9	18	1.24	5.5e-9
	2^{-6}	17	4.07	8.0e-9	11	2.86	4.3e-9	19	4.62	1.8e-9

Table 4.5: Iteration counts, elapsed time (in seconds), and relative error for left-preconditioned GMRES with a relative residual tolerance of 10^{-8} for a 2D diffusion equation with variable coefficients with s -stage Radau IIA methods with preconditioners: Gauss–Seidel, LD, and DU. The time-step is given by $h_t = h^{\frac{2}{2s-1}}$. Preconditioners are applied via a single AMG V-Cycle for all of the block subsolves.

upper triangular) we approximate application of the preconditioners by solving the block systems using forward or backward substitution. For each diagonal subsolve, we use a single AMG V-Cycle. This allows for faster solves with regards to the preconditioner, which translates to overall faster solve times. For more details on the specifics on this process, see [12].

4.3.1. Diffusion and Pennes equations. For the parabolic problems, we again employ the Radau IIA IRK method timestepper. Due to the established results for the diffusion problem in [8, 12, 13], we focus on the Pennes problem with both constant and variable coefficients.

Results are shown in Table 4.6. Iteration counts for all three preconditioners depend weakly on h and on s . For fixed s , solve time increases by a factor of $\sim 3 - 4$ as h is halved, as expected in a 2D problem with h -independent iteration count. Acceptable errors are achieved, comparable to the residual tolerance imposed. Once again, the LD preconditioner usually outperforms the other two.

4.3.2. Wave and Klein–Gordon equations. Finally, we investigate the performance of the top three preconditioners in GMRES as applied to the wave and Klein–Gordon equations with constant and variable coefficients. As before, the Gauss–Legendre IRKN method is used for these problem. For the wave equation, we look at $h = 2^{-5}$ and 2^{-6} , while for the Klein–Gordon equation we consider $h = 2^{-8}$ and 2^{-9} . Results for the wave equation are shown in Table 4.7; those for the Klein–Gordon equation are shown in 4.8. For all three preconditioners we see a significant increase in iteration count and solve time as s is increased, but all show little or no sensitivity to h . Interestingly, unlike in the parabolic problems, we see the LD and DU preconditioners outperform the GSL preconditioner, with the DU being slightly better than the LD preconditioner. Again, tolerable accuracy is achieved.

		$\mathcal{P}_{GSL}^{-1}\mathcal{A}$			$\mathcal{P}_{LD}^{-1}\mathcal{A}$			$\mathcal{P}_{DU}^{-1}\mathcal{A}$				
RIIA	h	it.	t	err.	it.	t	err.	it.	t	err.		
Constant Coef.	s=2	2^{-5}	8	0.11	4.5e-8	5	0.08	3.6e-8	6	0.09	8.7e-9	
		2^{-6}	8	0.55	4.1e-8	5	0.39	2.6e-8	6	0.44	4.2e-9	
	s=3	2^{-5}	10	0.31	4.8e-8	9	0.33	8.2e-9	8	0.26	3.8e-9	
		2^{-6}	14	1.53	4.5e-9	11	1.29	1.4e-9	9	0.97	1.8e-7	
	s=4	2^{-5}	13	0.56	6.4e-7	11	0.54	2.6e-9	15	0.70	1.3e-8	
		2^{-6}	19	2.86	2.9e-9	14	2.25	3.6e-10	15	2.36	5.2e-8	
	s=5	2^{-5}	20	1.19	5.6e-9	10	0.61	5.6e-7	18	1.09	3.4e-8	
		2^{-6}	23	4.47	2.9e-9	14	3.03	5.4e-9	20	4.08	1.5e-8	
	Variable Coef.	s=2	2^{-5}	11	0.21	7.8e-10	5	0.09	8.9e-9	6	0.12	1.7e-9
			2^{-6}	8	0.82	1.1e-8	7	0.68	4.5e-10	7	0.67	2.8e-10
s=3		2^{-5}	13	0.48	2.2e-9	9	0.38	6.4e-10	10	0.41	5.3e-9	
		2^{-6}	11	1.59	8.2e-9	8	1.24	1.7e-9	10	1.48	3.9e-9	
s=4		2^{-5}	19	0.97	1.0e-9	10	0.57	4.3e-9	16	0.85	1.6e-9	
		2^{-6}	16	2.91	4.3e-9	10	2.05	1.5e-9	15	2.85	4.7e-9	
s=5		2^{-5}	19	1.25	4.1e-9	11	0.81	5.2e-9	19	1.29	1.3e-9	
		2^{-6}	17	4.06	7.9e-9	11	2.86	4.3e-9	20	4.81	1.4e-9	

Table 4.6: Iteration counts, elapsed time (in seconds), and relative error for left-preconditioned GMRES with a relative residual tolerance of 10^{-8} for a 2D Pennes Equation ($\beta > 0$) with constant coefficients (top) and variable coefficients (bottom) with s -stage Radau IIA methods with preconditioners: Gauss–Seidel, LD, and DU. The time-step is given by $h_t = h^{\frac{2}{2s-1}}$.

5. Conclusions. In this paper, we developed a unified formulation and analysis of the stage equations for implicit Runge–Kutta and Runge–Kutta–Nyström timesteppers applied to a large class of parabolic and hyperbolic equations of importance in applications. With this unified approach, we were able to prove the order-optimality of many preconditioners for these problems, including those in [8, 13] and [12]. In particular, the order optimality of Rana’s LD preconditioner for any problem is a new result. We also performed numerical experiments to investigate the dependence on timestep and mesh size in practice, the effect on these preconditioners on the spectrum and field of values of the system, and the influence on GMRES solve time. Since our formulation encompasses problems with variable coefficients, we also investigated such problems.

We found in all cases that preconditioner performance was only slightly influenced by whether the problem’s coefficients were variable or constant. For the parabolic problems with IRK (Radau IIA) timesteppers, we found results consistent with those of [12], namely that the LD preconditioner consistently outperforms the alternatives. For the hyperbolic problems with IRKN (Gauss–Legendre based) timesteppers we found that the DU preconditioner — which hadn’t been very effective on parabolic problems — was marginally superior to the LD preconditioner, and both were markedly

		$\mathcal{P}_{GSL}^{-1}\mathcal{A}$			$\mathcal{P}_{LD}^{-1}\mathcal{A}$			$\mathcal{P}_{DU}^{-1}\mathcal{A}$				
	GL	h	it.	t	err.	it.	t	err.	it.	t	err.	
Constant Coef.	s=2	2^{-5}	14	0.19	5.4e-8	7	0.10	8.5e-8	10	0.15	4.7e-9	
		2^{-6}	14	0.84	3.3e-8	10	0.67	6.6e-9	10	0.66	3.6e-9	
	s=3	2^{-5}	16	0.47	2.0e-7	8	0.29	8.9e-9	8	0.25	8.5e-8	
		2^{-6}	22	2.06	8.2e-9	7	0.81	1.3e-8	8	0.81	5.1e-8	
	s=4	2^{-5}	66	2.71	3.5e-7	29	1.24	1.1e-8	28	1.18	2.1e-8	
		2^{-6}	60	7.60	7.8e-7	27	3.66	8.4e-9	20	2.60	5.6e-7	
	s=5	2^{-5}	204	11.17	2.3e-8	31	1.80	4.5e-8	27	1.55	4.5e-6	
		2^{-6}	211	35.95	3.4e-8	31	5.54	3.5e-8	28	4.95	1.5e-6	
	Variable Coef.	s=2	2^{-5}	12	0.15	3.8e-8	7	0.10	5.9e-8	10	0.15	6.5e-7
			2^{-6}	11	0.67	2.1e-7	6	0.46	7.5e-8	6	0.45	9.9e-8
s=3		2^{-5}	19	0.71	2.0e-8	9	0.38	3.1e-10	10	0.41	5.1e-9	
		2^{-6}	16	2.40	2.1e-8	6	0.95	1.4e-8	10	1.57	3.0e-9	
s=4		2^{-5}	61	2.53	1.6e-7	25	1.18	1.1e-8	29	1.38	9.9e-9	
		2^{-6}	49	7.30	9.2e-7	20	3.63	1.2e-8	27	4.76	6.9e-9	
s=5		2^{-5}	164	9.05	5.8e-8	27	1.70	3.7e-8	34	2.16	1.8e-7	
		2^{-6}	149	29.25	5.1e-7	35	6.11	3.4e-8	31	7.58	7.8e-8	

Table 4.7: Iteration counts, elapsed time (in seconds), and relative error for left-preconditioned GMRES with a relative residual tolerance of 10^{-8} for a 2D wave equation ($\beta = 0$) with constant coefficients (top) and variable coefficients (bottom) with s -stage Gauss–Legendre methods with preconditioners: Gauss–Seidel, LD, and DU. The time step is given by $h_t = h^{\frac{1}{s}}$.

superior to the Gauss–Seidel preconditioner.

Finally, we mention that while the class of problems considered here is large, the restriction to non-negative coefficients $\beta(\mathbf{r}) \geq 0$ may be an issue for linearizations of nonlinear problems, in which a stage equation will have coefficients involving functions of previous Newton iterates, which may not respect that restriction. Furthermore, our analysis does not include the effect of advective terms $\mathbf{b} \cdot \nabla u$, which will be important in some applications. In [12], Rana *et al.* found that the LD preconditioner performed well in the presence of an advective term, but we don't yet have theoretical understanding of why it works well for those problems. Experimental and theoretical investigation of these issues will be the subject of future papers.

REFERENCES

- [1] I. BABUSKA AND A. K. AZIZ, *Survey lectures on the mathematical foundations on the finite element method*, Academic Press, New York, (1972), pp. 3–363.
- [2] N. BELL, L. N. OLSON, AND J. SHRODER, *PyAMG: Algebraic multigrid solvers in python*, 2022.
- [3] E. HAIRER, *Unconditionally stable methods for second order differential equations*, BIT Numerical mathematics, 32 (1979), pp. 373–379.

		$\mathcal{P}_{GSL}^{-1}\mathcal{A}$				$\mathcal{P}_{LD}^{-1}\mathcal{A}$			$\mathcal{P}_{DU}^{-1}\mathcal{A}$			
GL		h	it.	t	err.	it.	t	err.	it.	t	err.	
Constant Coef.	s=2	2^{-8}	4	0.66	1.0e-8	3	0.64	7.8e-9	3	0.64	1.9e-8	
		2^{-9}	4	2.47	1.9e-8	3	2.55	1.3e-8	3	2.58	3.2e-8	
	s=3	2^{-8}	7	2.40	4.7e-9	5	1.97	8.6e-9	5	1.91	5.3e-9	
		2^{-9}	5	11.21	1.2e-8	4	11.45	6.5e-8	4	9.68	8.1e-9	
	s=4	2^{-8}	40	14.86	4.8e-9	11	4.75	3.1e-8	10	4.36	9.1e-9	
		2^{-9}	38	100.1	4.3e-9	11	34.30	6.0e-8	15	46.87	1.7e-9	
	s=5	2^{-8}	100	47.07	1.0e-8	14	7.45	6.5e-8	14	7.46	2.7e-8	
		2^{-9}	111	218.2	1.7e-8	18	39.00	1.3e-9	16	35.44	1.3e-8	
	Variable Coef.	s=2	2^{-8}	5	0.74	7.9e-9	3	0.64	1.2e-8	3	0.63	2.3e-8
			2^{-9}	4	2.53	5.7e-8	3	2.69	1.8e-8	3	2.66	5.1e-8
s=3		2^{-8}	12	3.82	2.7e-9	4	1.49	1.7e-8	5	1.93	7.6e-9	
		2^{-9}	9	11.46	3.1e-9	4	7.22	7.2e-8	4	5.89	2.3e-8	
s=4		2^{-8}	40	15.13	7.2e-9	12	5.23	5.6e-8	15	6.69	1.3e-9	
		2^{-9}	39	95.14	4.2e-9	12	21.10	4.7e-8	10	18.36	2.9e-8	
s=5		2^{-8}	100	48.32	1.8e-8	18	9.45	4.3e-8	16	8.64	2.0e-8	
		2^{-9}	111	221.4	1.7e-8	17	37.08	5.8e-8	16	34.92	1.8e-8	

Table 4.8: Iteration counts, elapsed time (in seconds), and relative error for left-preconditioned GMRES to converge to a residual tolerance of 10^{-8} for a 2D Klein–Gordon equation ($\beta > 0$) with constant coefficients (top) and variable coefficients (bottom) with s -stage Gauss–Legendre methods with preconditioners: Gauss–Seidel, LD, and DU. The time-step is given by $h_t = h^{\frac{1}{s}}$.

- [4] P. HOUWEN, B. SOMMEIJER, AND N. H. CONG, *Stability of collocation-based Runge–Kutta–Nyström methods*, BIT Numerical mathematics, 31 (1991), pp. 469–481.
- [5] E. JONES, T. OLIPHANT, AND P. PETERSON, *SciPy: Open source scientific tools for Python*, 2001.
- [6] J. LIESEN AND P. TICH’Y, *The field of values bound on ideal gmres*, arXiv: Numerical Analysis, (2012).
- [7] K. LONG, R. KIRBY, AND B. VAN BLOEMEN WAANDERS, *Unified embedded parallel finite element computations via software-based frechet differentiation*, SIAM Journal on Scientific Computation, (2010), pp. 3323–3351.
- [8] K.-A. MARDAL, T. NILSSEN, AND G. STAFF, *Order-optimal preconditioners for implicit Runge–Kutta schemes applied to parabolic PDEs*, SIAM J. Scientific Computing, 29 (2007), pp. 361–375.
- [9] T. NILSSEN, *Weakly positive definite matrices*, tech. rep., Simula Research Laboratory, Lysaker Norway, 07 2005.
- [10] J. T. ODEN AND J. N. REDDY, *An introduction to the mathematical theory of finite elements*, Courier Corporation, 2012.
- [11] H. H. PENNES, *Analysis of tissue and arterial blood temperatures in the resting human forearm*, Journal of applied physiology, 1 (1948), pp. 93–122.
- [12] M. M. RANA, V. E. HOWLE, K. LONG, A. MEEK, AND W. MILESTONE, *A new block preconditioner for implicit Runge–Kutta methods for parabolic PDE problems*, SIAM J. Scientific Computing, 43 (2021).
- [13] G. STAFF, K.-A. MARDAL, AND T. NILSSEN, *Preconditioning of fully implicit Runge–Kutta schemes for parabolic PDEs*, Modeling, Identification and Control, 27 (2006).

Appendix A. Proof of Theorem 3.1. The proof of our Theorem 3.1 follows the outline of the proof of the special case in [8], with the appropriate modifications for our more general problem. At each timestep, we solve the equation $\mathcal{A}\mathbf{u}^n = \mathbf{f}^n$, where \mathcal{A} and \mathbf{f}^n were defined in (2.3) and (2.1). We introduce the bilinear functional $a(\mathbf{u}, \mathbf{v}) := \langle \mathcal{A}\mathbf{u}, \mathbf{v} \rangle_{\mathbf{V}}$. With few restrictions on the structure of the Butcher coefficient matrix A in the operator \mathcal{A} defined in (2.3), we cannot assume $a(\cdot, \cdot)$ is coercive; we therefore need the Babuska–Aziz theorem [1, 10].

Throughout this section, norms and inner products are assumed to be on V or \mathbf{V} unless otherwise specified.

THEOREM A.1. (*Babuska–Aziz*) *The linear map $\mathcal{A} : \mathbf{V} \rightarrow \mathbf{V}^*$ is an isomorphism if the following conditions are satisfied:*

1. [*Boundedness*] *There exists a c_1 independent of h_t such that:*

$$|a(\mathbf{u}, \mathbf{v})| \leq c_1 \|\mathbf{u}\| \|\mathbf{v}\|, \quad \forall \mathbf{u}, \mathbf{v} \in \mathbf{V}.$$

2. [*inf-sup*] *There exists a c_2 independent of h_t such that*

$$\sup_{\mathbf{v} \in \mathbf{V}} \frac{|a(\mathbf{u}, \mathbf{v})|}{\|\mathbf{v}\|} \geq \frac{1}{c_2} \|\mathbf{u}\|, \quad \mathbf{u} \in \mathbf{V}.$$

3. *For $\mathbf{v} \in \mathbf{V} \setminus \mathbf{0}$ there exists $\mathbf{u} \in \mathbf{V}$ such that*

$$a(\mathbf{u}, \mathbf{v}) \neq 0.$$

The proof of Theorem 3.1 therefore reduces to showing that \mathcal{A} satisfies the conditions in Theorem A.1. The essential idea is that we can follow the path laid out by [8], replacing operations such as $\langle \nabla \mathbf{u}, \nabla \mathbf{v} \rangle$ by $\langle \mathbf{u}, \mathbf{v} \rangle_{\mathbf{H}_0^1}$; the logic is the same but the details differ. We require the following lemma, proved in [9].

LEMMA A.2. *Let $A \in \mathbb{R}^{s \times s}$ be a weakly positive definite matrix, and let $C \in \mathbb{R}^{s \times s}$ be the associated positive definite matrix of A . Then, there exists $\epsilon > 0$ such that for all $\mathbf{x} \in \mathbb{R}^s$, we have*

$$\begin{aligned} \mathbf{x}^T C \mathbf{x} &\geq \epsilon \|\mathbf{x}\|_2^2 \\ \mathbf{x}^T C A \mathbf{x} &\geq \epsilon \|\mathbf{x}\|_2^2. \end{aligned}$$

We now prove Theorem 3.1.

Proof. We begin with the boundedness condition. Let $a_{\max} = \max(\max_{i,j} |a_{ij}|, 1)$.

Then compute a bound on $|a(\mathbf{u}, \mathbf{v})|$ as follows:

$$\begin{aligned}
|a(\mathbf{u}, \mathbf{v})| &= |\langle \mathcal{A}\mathbf{u}, \mathbf{v} \rangle| = \left| \langle \mathbf{u}, \mathbf{v} \rangle_{\mathbf{L}^2} + h_t^\mu \sum_{i=1}^s \sum_{j=1}^s a_{ij} \langle u_j, v_i \rangle_{H_0^1} \right| \\
&\leq |\langle \mathbf{u}, \mathbf{v} \rangle_{\mathbf{L}^2}| + h_t^\mu \sum_{i,j \leq s} |a_{ij}| \left| \langle u_j, v_i \rangle_{H_0^1} \right| \\
&\leq a_{\max} \left[\|\mathbf{u}\|_{\mathbf{L}^2} \|\mathbf{v}\|_{\mathbf{L}^2} + h_t^\mu \sum_{i,j \leq s} \|u_j\|_{H_0^1} \|v_i\|_{H_0^1} \right] \\
&\leq a_{\max} s \left[\|\mathbf{u}\|_{\mathbf{L}^2} \|\mathbf{v}\|_{\mathbf{L}^2} + h_t^\mu \|\mathbf{u}\|_{\mathbf{H}_0^1} \|\mathbf{v}\|_{\mathbf{H}_0^1} \right] \\
&\leq a_{\max} s \left(\|\mathbf{u}\|_{\mathbf{L}^2}^2 + h_t^\mu \|\mathbf{u}\|_{\mathbf{H}_0^1}^2 \right)^{1/2} \left(\|\mathbf{v}\|_{\mathbf{L}^2}^2 + h_t^\mu \|\mathbf{v}\|_{\mathbf{H}_0^1}^2 \right)^{1/2} \\
&\leq a_{\max} s \|\mathbf{u}\|_{\mathbf{V}} \|\mathbf{v}\|_{\mathbf{V}}.
\end{aligned}$$

Set c_1 to $a_{\max} s$, and condition 1 (boundedness) is met.

We now establish condition 2, the inf-sup condition. If $\mathbf{u} = \mathbf{0}$, the result is immediate. Otherwise, let $\mathbf{u} \in \mathbf{V} \setminus \mathbf{0}$, set $\mathbf{v} = C^T \mathbf{u}$, and define $\epsilon \in \mathbb{R}$ by

$$\epsilon := \min \left(\min_{\|\mathbf{x}\|=1} \mathbf{x}^T C \mathbf{x}, \min_{\|\mathbf{x}\|=1} \mathbf{x}^T C A \mathbf{x} \right).$$

Now compute:

$$\begin{aligned}
\sup_{\mathbf{v} \in \mathbf{V}} \frac{\langle \mathcal{A}\mathbf{u}, \mathbf{v} \rangle}{\|\mathbf{u}\| \|\mathbf{v}\|} &\geq \frac{\langle \mathcal{A}\mathbf{u}, C^T \mathbf{u} \rangle}{\|\mathbf{u}\| \|C^T \mathbf{u}\|} \\
&= \frac{\langle C \mathcal{A}\mathbf{u}, \mathbf{u} \rangle}{\|\mathbf{u}\| \|C^T \mathbf{u}\|} \\
&= \frac{\langle C (\mathbb{I}^{s \times s} \otimes \mathcal{I} + h_t^\mu A \otimes \mathcal{K}) \mathbf{u}, \mathbf{u} \rangle}{\|\mathbf{u}\| \|C^T \mathbf{u}\|} \\
&= \frac{1}{\|\mathbf{u}\| \|C^T \mathbf{u}\|} \left[\langle C \mathbf{u}, \mathbf{u} \rangle_{\mathbf{L}^2} + h_t^\mu \langle C \mathcal{A}\mathbf{u}, \mathbf{u} \rangle_{\mathbf{H}_0^1} \right].
\end{aligned}$$

From Lemma A.2, we have

$$\begin{aligned}
\frac{1}{\|\mathbf{u}\| \|C^T \mathbf{u}\|} \left[\langle C \mathbf{u}, \mathbf{u} \rangle_{\mathbf{L}^2} + h_t^\mu \langle C \mathcal{A}\mathbf{u}, \mathbf{u} \rangle_{\mathbf{H}_0^1} \right] &\geq \frac{\epsilon}{\|\mathbf{u}\| \|C^T \mathbf{u}\|} \left[\|\mathbf{u}\|_{\mathbf{L}^2}^2 + h_t^\mu \|\mathbf{u}\|_{\mathbf{H}_0^1}^2 \right] \\
&= \frac{\epsilon \|\mathbf{u}\|}{\|C^T \mathbf{u}\|} \geq \frac{\epsilon}{\|C^T\|} > 0.
\end{aligned}$$

Therefore, $\sup_{\mathbf{v} \in \mathbf{V}} \frac{\langle \mathcal{A}\mathbf{u}, \mathbf{v} \rangle}{\|\mathbf{v}\|} \geq \frac{1}{c_2} \|\mathbf{u}\|$, where $c_2^{-1} = \epsilon / \|C^T\| > 0$, and the inf-sup condition is met.

Finally, we prove the third condition. As in [8]: since A^T and A share the same set of eigenvalues, it follows that A^T must also be weakly positive definite (since no eigenvalues of A^T are negative and real). Hence there exists a positive definite matrix D such that DA^T is positive definite as well. We choose an arbitrary $\mathbf{v} \in \mathbf{V} \setminus \mathbf{0}$ and

define $\mathbf{u} = D^T \mathbf{v}$. Then

$$\begin{aligned} \mathcal{A}(\mathbf{u}, \mathbf{v}) &= \langle AD^T \mathbf{v}, \mathbf{v} \rangle = \langle (\mathbb{I}^{s \times s} \otimes \mathcal{I} + h_t^\mu A \otimes \mathcal{K}) D^T \mathbf{v}, \mathbf{v} \rangle \\ &= \langle D^T \mathbf{v}, \mathbf{v} \rangle_{\mathbf{L}^2} + h_t^\mu \langle AD^T \otimes \mathcal{K} \mathbf{v}, \mathbf{v} \rangle_{\mathbf{L}^2} \\ &= \langle \mathbf{v}, D\mathbf{v} \rangle_{L^2} + h_t^\mu \langle \mathbf{v}, DA^T \mathbf{v} \rangle_{\mathbf{H}_0^1} \end{aligned}$$

which is strictly positive since D and DA^T are positive definite, the operations $\langle \cdot, \cdot \rangle_{\mathbf{L}^2}$ and $\langle \cdot, \cdot \rangle_{\mathbf{H}_0^1}$ are positive definite and (at least) positive semidefinite respectively, and $\mathbf{v} \neq \mathbf{0}$. The third condition is met and the proof is complete. \square

Appendix B. Some Specific Preconditioners. Here, we define the preconditioners used in Section 4 to precondition the system $\mathbb{I}^{s \times s} \otimes M + h_t^p A \otimes F$:

$$\begin{aligned} \mathcal{P}_J &:= \mathbb{I}^{s \times s} \otimes M + h_t^p P_J \otimes F \\ \mathcal{P}_{GSL} &:= \mathbb{I}^{s \times s} \otimes M + h_t^p P_{GSL} \otimes F \\ \mathcal{P}_{TRIU} &:= \mathbb{I}^{s \times s} \otimes M + h_t^p P_{TRIU} \otimes F, \end{aligned}$$

where P_J , P_{GSL} , and P_{TRIU} are the diagonal, lower triangular part, and upper triangular part of A , respectively.

Let $A = LDU$ be the LDU factorization of A . Now set $P_{LD} = LD$ and $P_{DU} = DU$ and define the remaining preconditioners as

$$\begin{aligned} \mathcal{P}_{LD} &:= \mathbb{I}^{s \times s} \otimes M + h_t^p P_{LD} \otimes F \\ \mathcal{P}_{DU} &:= \mathbb{I}^{s \times s} \otimes M + h_t^p P_{DU} \otimes F. \end{aligned}$$